Available online at www.sciencedirect.com
ScienceDirect
International Journal of Heat and Mass Transfer 50 (2007) 4652–4660
International Journal of HEAT and MASS TRANSFER
www.elsevier.com/locate/ijhmt

Bioconvection of gravitactic micro-organisms in rectangular enclosures

M. Taheri, E. Bilgen *

Ecole Polytechnique, University of Montreal, C.P 6079, centre-ville, Montréal, QC, Canada H3C 3A7

Received 17 November 2006; received in revised form 7 March 2007
Available online 30 April 2007

Abstract

This paper investigates the gravitactic bioconvection in rectangular enclosures. The governing equations are the continuity, the Navier–Stokes equations with the Boussinesq approximation and the diffusion equation for the motile micro-organisms. The control volume method is used to solve numerically the complete set of governing equations. The effects of bioconvection Peclet number from 0.1 to 10 and the aspect ratio from 1 to 5 are investigated on the onset of bioconvection. It was found that the bifurcation was subcritical in all cases. The critical Rayleigh number is decreased with increasing bioconvection Peclet number and with increasing aspect ratio.

Keywords: Bioconvection; Gravitactic micro-organisms; Bifurcation; Pattern formation

1. Introduction

Bioconvection is the spontaneous pattern formation in suspensions of micro-organisms, which are little denser than water and move randomly, but on average upwardly against gravity. Up swimming of micro-organisms is generally a response to an external force field such as gravity (gravitaxis or geotaxis), light source (phototaxis), biochemical stimulus such as gradient of oxygen concentration (chemotaxis) and torques due to gravity and shear (gyrotaxis). Due to up swimming, the top layer of the suspension becomes denser than the layer below, resulting in an unstable density distribution. This may lead to a convective instability and formation of convection patterns similar to the patterns observed in the Rayleigh–Bénard convection. Theoretical models of bioconvection for different types of motile micro-organisms have been developed in various recent publications, including Metcalfe and Pedley [1], Hillesdon and Pedley [2] and Hill et al. [3]. For a review of the fundamental work in this area, see Pedley and Kessler [4] and Hill and Pedley [5].

Rational continuum models for a suspension of purely gravitactic micro-organisms have been formulated and analyzed by Childress et al. [6]. The formulation includes the Navier–Stokes equations with the Boussinesq approximation for an incompressible fluid and the micro-organisms conservation equation. A numerical study based on the equations derived by Childress et al. [6] was presented by Fujita and Watanabe [7]. They discretized the equations using finite difference method with a spatially staggered grid. They found that the system of bioconvection can lead into chaotic behavior via a sequence of bifurcations by increasing the Rayleigh number. The preferred wave number of gravitactic bioconvection in a rectangular cavity was studied by Harashima et al. [8] who carried out numerical experiments to show that the system evolves in the direction of intensifying downward advection of micro-organisms and reducing the total potential energy of the system. Ghorai and Hill [9] studied gyrotactic bioconvection, using a vorticity-stream function formulation of the basic model, which was first introduced by Pedley et al. [10]. The development and instabilities of a single, two-dimensional gyrotactic plume and a periodic array of such plumes were examined in Ghorai and Hill [9,11]. They investigated numerically the existence and stability of a plume in a suspension of gyrotactic swimming micro-organisms, *Chlamydomonas nivalis*, in a deep and narrow

* Corresponding author. Tel.: +514 340 4711x4579; fax: +514 340 5917.
E-mail address: bilgen@polymtl.ca (E. Bilgen).

0017-9310/$ - see front matter © 2007 Elsevier Ltd. All rights reserved.
doi:10.1016/j.ijheatmasstransfer.2007.03.009

Nomenclature

A	cavity aspect ratio, $A = L/H$
D_c	cell diffusivity
g	gravitational acceleration
H	cavity height
$\vec{J}$	dimensionless flux of micro-organisms
$\vec{k}$	unit vector
L	cavity width
n	dimensionless cell concentration
$\bar{n}$	average cell concentration
$\vec{n}$	unit normal vector to the boundaries
p	dimensionless pressure
Pe	bioconvection Peclet number, $Pe = HV_c/D_c$
Ra	bioconvection Rayleigh number, $Ra = g\vartheta\Delta\rho\bar{n}H^3/\rho\nu D_c$
Sc	Schmidt number, $Sc = \nu/D_c$
t	dimensionless time
$\vec{u}$	dimensionless fluid velocity
V_c	gravitactic cell velocity
x, y	dimensionless coordinate system

Greek symbols

α	thermal diffusivity
μ	dynamic viscosity of the suspension
ν	kinematic viscosity of the suspension
ρ_c	cell density
ρ_w	water density
$\Delta\rho$	difference between cell and water densities, $\Delta\rho = \rho_c - \rho_w$
ϑ	cell volume
ψ	dimensionless stream function
ω	dimensionless vorticity

Superscripts

$'$	dimensional variable
sub	subcritical
sup	supercritical

chamber with stress-free side walls. Their governing parameters were, in our notation, $Sc = 20$, $Pe = 5$–20, $A = 1$–0.125, i.e., square to tall, narrow enclosures. They carried out a parametric study to determine effects of gyrotactic number and cell swimming speed, and the instability mechanism. They carried out also a linear stability analysis at small gyrotactic numbers and found good agreement between the numerical and the linear stability analysis results [9]. Bees and Hill [12] carried out a study by weakly non-linear theory and showed that in gyrotactic swimming micro-organisms in a deep suspension, the bifurcation to instability was supercritical. They found also that the linear theory was adequate to predict the pattern formation, i.e., the first plumes to appear in initially a well mixed deep suspension of gyrotactic micro-organisms.

The onset of bioconvection and the mechanism of bifurcation are studied by using linear stability theory, nonlinear theory and numerical methods (e.g., [4]). For gravitaxis bioconvection, using weakly nonlinear theory Childress and Spiegel [13] found that the bifurcation in bioconvection of gravitactic micro-organisms in a horizontal fluid layer was subcritical. Recently, Alloui et al. [14] studied numerically bioconvection and pattern formation of gravitactic micro-organisms in a vertical cylinder, with the aspect ratio of 1 and 0.1, i.e., square and tall enclosures. They found that the pattern formation at low Peclet numbers was analogous to the Rayleigh–Bénard convection, i.e., the bifurcation was supercritical, while at high Peclet numbers it was subcritical. In contrast, it is found that pattern formation in gyrotaxis bioconvection in tall enclosures was through supercritical bifurcation [9,12].

We focus in this paper on gravitactic bioconvection developed in a suspension of gravitactic micro-organisms, like *paramecium* and *tetrahymena*, in square to shallow enclosures. The governing parameters are $Sc = 1$, $Pe = 0.1$–10 and $A = 1$–5. We will obtain numerical solutions to the governing equations of the continuity, the full Navier–Stokes and the cell concentration at critical conditions for the onset of convection. Our aim is to investigate the effects of the aspect ratio and Peclet number on the onset and development of bioconvection.

2. Mathematical formulation

The system consists of a suspension of gravitactic micro-organisms enclosed in a two-dimensional rectangular cavity of width L and height H referred to Cartesian coordinates (x', y') with the y' axis pointing vertically upwards (Fig. 1). Initially we have a uniform concentration distribution $\bar{n}$ and each cell has a volume ϑ and density ρ_c. Assuming that the suspension is incompressible and introducing the stream function ψ' and the vorticity ω', we get

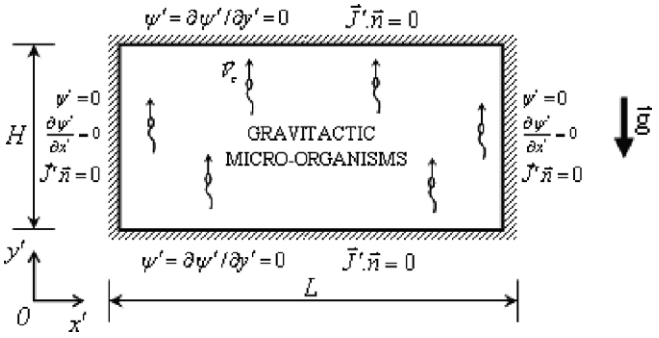

Fig. 1. Schematic diagram of the computational domain and boundary conditions.

$$\vec{u}' = (\partial\psi'/\partial y', -\partial\psi'/\partial x') \tag{1}$$

$$\omega' = -\nabla^2\psi' \tag{2}$$

The Boussinesq approximation assumes that all physical properties are constant except for the density in the buoyancy term, which may be expressed as a linear function of cell concentration

$$\rho = \rho_w + (\rho_c - \rho_w)n'\vartheta = \rho_w\left(1 + \vartheta\frac{\Delta\rho}{\rho_w}n'\right) \tag{3}$$

where ρ is the density of the suspension, ρ_w and ρ_c the density of the fluid and of the cells, respectively.

The momentum equation under the Boussinesq approximation leads to the vorticity equation

$$\frac{\partial\omega'}{\partial t'} + \nabla\cdot(\omega'\vec{u}') = \nu\nabla^2\omega' - g\vartheta\frac{\Delta\rho}{\rho_w}\frac{\partial n'}{\partial x'} \tag{4}$$

Here, ν is the kinematic viscosity of the suspension, which is assumed to be that of the fluid.

The cell concentration can be described by the equation

$$\frac{\partial n'}{\partial t'} = -\nabla\cdot\vec{J}' \tag{5}$$

where the flux of the cells is

$$\vec{J}' = (\vec{u}' + V_c\vec{k})n' - D_c\nabla n' \tag{6}$$

with n' being the number of cells in a unit volume, V_c the upward velocity, $\vec{k}$ vertical unit vector and D_c the diffusion coefficient of the cells.

We impose rigid, non-slip boundary conditions at the top, bottom and side walls. Also there is no flux of cells through the walls (Fig. 1). Hence

$$\psi' = 0, \quad \frac{\partial\psi'}{\partial x'} = 0 \quad \text{and} \quad \vec{J}'\cdot\vec{n} = 0 \quad \text{at } x' = 0, L \tag{7}$$

$$\psi' = 0, \quad \frac{\partial\psi'}{\partial y'} = 0 \quad \text{and} \quad \vec{J}'\cdot\vec{n} = 0 \quad \text{at } y' = 0, H \tag{8}$$

where $\vec{n}$ is the unit vector normal to the boundary.

Length is scaled on the height H, time on the diffusive scale H^2/D_c, velocity on D_c/H, and the concentration on the mean concentration $\bar{n}$. The resulting system of coupled equations is

$$\omega = -\nabla^2\psi \tag{9}$$

$$\frac{\partial\omega}{\partial t} + \nabla\cdot(\omega\vec{u}) = Sc\nabla^2\omega - ScRa\frac{\partial n}{\partial x} \tag{10}$$

$$\frac{\partial n}{\partial t} = -\nabla\cdot\vec{J} \tag{11}$$

where the flux of the cells is

$$\vec{J} = (\vec{u} + Pe\vec{k})n - \nabla n \tag{12}$$

Here, $Sc = \nu/D_c$ is the Schmidt number, $Pe = V_cH/D_c$ the bioconvection Peclet number and $Ra = g\vartheta\bar{n}\Delta\rho H^3/\rho\nu D_c$ the bioconvection Rayleigh number.

Eqs. (9)–(11) are subjected to the boundary conditions

$$\begin{cases} \psi = 0, \frac{\partial\psi}{\partial x} = 0 \quad \text{and} \quad -\frac{\partial n}{\partial x} = 0 \quad \text{at } x = 0, A \\ \psi = 0, \frac{\partial\psi}{\partial y} = 0 \quad \text{and} \quad nPe - \frac{\partial n}{\partial y} = 0 \quad \text{at } y = 0, 1 \end{cases} \tag{13}$$

where $A = L/H$ is the aspect ratio of the cavity.

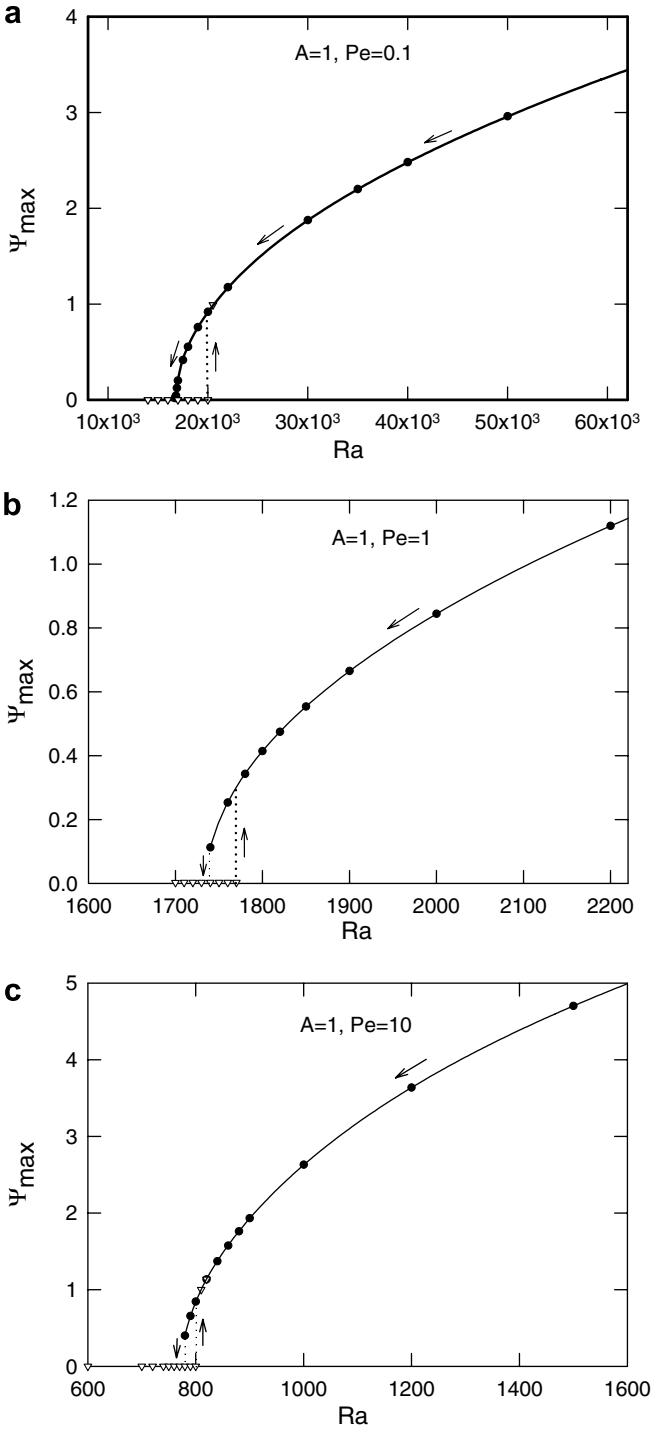

Fig. 2. Bifurcation diagrams for aspect ratio $A = 1$ and various bioconvection Peclet numbers. (a) $Pe = 0.1$; (b) $Pe = 1$ and (c) $Pe = 10$.

3. Numerical procedure

The control volume method of Patankar [15] is used to discretize governing Eqs. (9)–(12) with a uniform staggered grid with the stream function stored on one set of nodes and the vorticity and concentration stored on another set of nodes. The discretized equations are derived using the central differences for spatial derivatives and backward differences for time derivatives. A line-by-line tridiagonal matrix algorithm with relaxation is used in conjunction with iteration to solve the nonlinear discretized equations.

The validation of the code was done earlier [14], which is summarized here. Eqs. (9)–(11) with Eq. (13) possess a steady-state solution with $\psi = \omega = 0$, which is solved analytically and the results are compared to those obtained numerically using the present code. The agreement found was excellent for $Pe = 1$ and 10. Additionally, by using the present code, we simulated the Rayleigh–Bénard convection in a horizontal fluid layer heated from below by constant temperature and produced bifurcation diagram. We determined the critical Rayleigh number as 1708, consistent with the literature [16].

Uniform grid in x and y direction were used for all computations. Grid convergence was studied for the case of $A = 1$ and $Pe = 10$ with grid sizes from 11×11 to 151×151. Grid independence was achieved with grid size

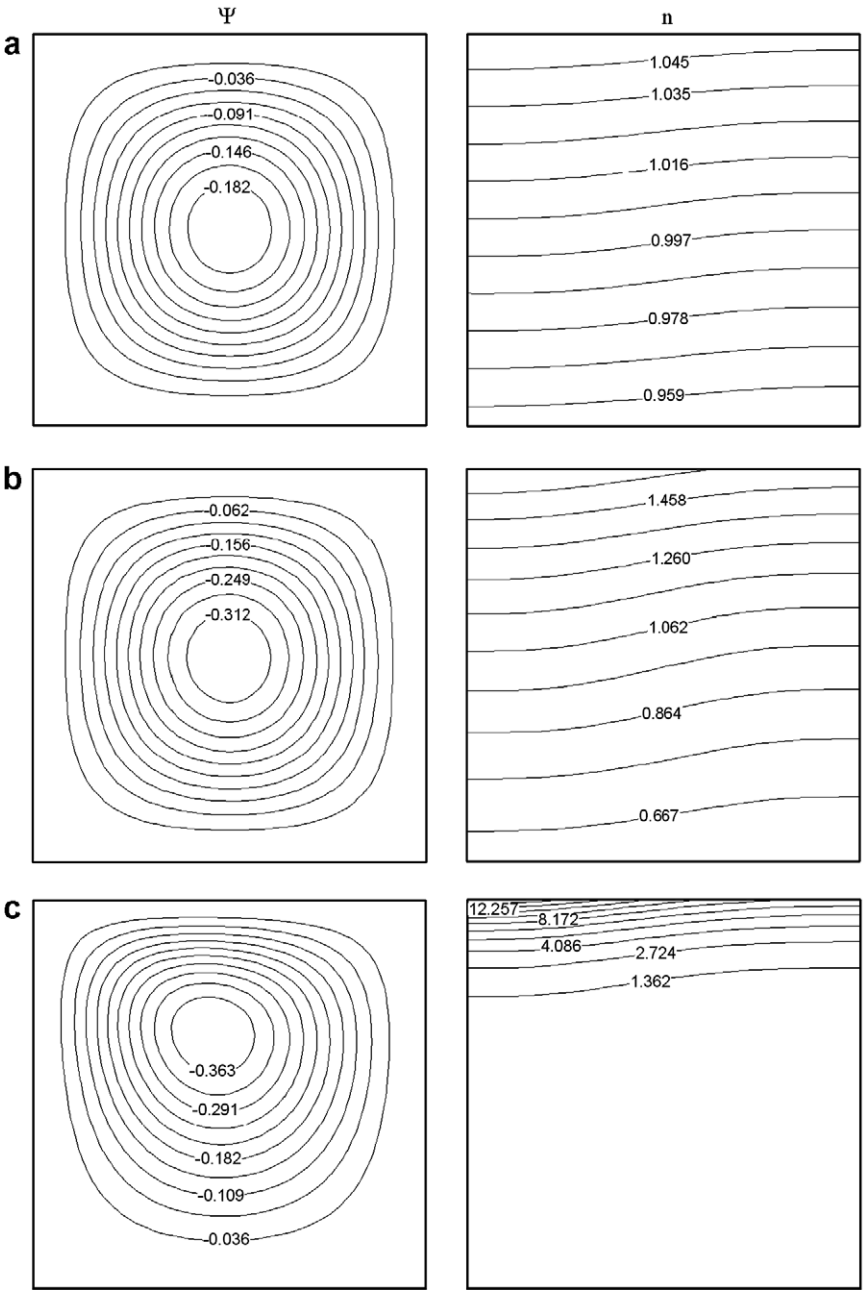

Fig. 3. Streamlines and isoconcentrations for $A = 1$ of Fig. 2. (a) $Pe = 0.1$, $Ra = 17000$; (b) $Pe = 1$, $Ra = 1780$ and (c) $Pe = 10$, $Ra = 780$.

of 51×51 within 0.1% in extremum stream function with reference to that of 151×151. Similar tests were done with the cavities having $A = 2$ and 5, and found that the grid size was satisfactory with the following grids: 51×101 for $A = 2$ and 51×251 for $A = 5$. The time step Δt was 0.02.

We consider that the convergence is reached when

$$\frac{|f_{i,j}^{k+1} - f_{i,j}^{k}|}{\max |f_{i,j}^{k}|} \leqslant \varepsilon \tag{14}$$

where f corresponds to the variables (ω, ψ, n) and ε is the prescribed tolerance, k is the iteration number, and i, j denote the grid points. The results were obtained with $\varepsilon = 10^{-6}$ and $k = t/\Delta t$ was variable depending on the convergence time t.

4. Results and discussion

Computations are performed for the following values of dimensionless parameters: Aspect ratio of $A = 1$, 2 and 5, the bioconvection Peclet number, $Pe = 0.1$, 1 and 10, the Schmidt number $Sc = 1$ and the Rayleigh number variable. Pe and Sc numbers correspond to bioconvection cases with typical micro-organisms (e.g., [17,18]): the diffusion coefficient $D_c = 5 \times 10^{-3}$–0.5×10^{-2} cm^2/s, the cell velocity $V_c = 7.5 \times 10^{-3}$–1×10^{-2} m/s, the cell density $\rho_c = (1.035\text{–}1.10)\rho$, the cell volume $\theta = 1 \times 10^{-12}$–$5 \times 10^{-10}$ cm^3, the cell concentration $= 8.44 \times 10^{5}$–1×10^{9} cell/cm^3. For example, for *paramecium caudatum* used in [17], $D_c = 5 \times 10^{-3}$–4.5×10^{-2} cm^2/s, $V_c = 3.2 \times 10^{-2}$–7.7×10^{-2} cm/s, $H = 0.1$ cm; we obtain $Sc = 0.22$–2 and $Pe = 0.07$–1.54.

The procedure of determining the critical Rayleigh number and bifurcation was: we begin the simulation with the diffusion state as initial condition, gradually increasing the Rayleigh number until convection arises. Rayleigh at which the convection begins corresponds to the supercritical Rayleigh number. We continue to obtain solutions at higher Rayleigh numbers with the solution at the previous, lower Rayleigh number as initial condition. Once the solution at the highest Rayleigh number is obtained, we proceed backward to obtain solutions at lower Rayleigh numbers using the solution at the previous, higher Rayleigh number as initial condition. As Ra is decreased, we continue to obtain solutions until the convection disappears suddenly at a certain value, which corresponds to the subcritical Rayleigh number. Thus, it is found that the bioconvection arises, as the Rayleigh number Ra is increased at a certain *supercritical* value, Ra^{sup}, and disappears suddenly as Ra is decreased at a certain *subcritical* value, Ra^{sub}. It is $Ra^{sub} < Ra^{sup}$. This behaviour is typical of a subcritical bifurcation. It has also been observed experimentally by Mogami et al. [18], who analyzed the temporal and spatial changes in bioconvection pattern with varying gravity. They found a lower threshold, i.e., a lower critical Rayleigh number, for decreasing gravity than for increasing gravity.

We present the results of case with $A = 1$ and $Pe = 0.1$, 1 and 10 in Fig. 2. For $Pe = 0.1$ in Fig. 2a, we obtain $Ra_c^{sub} = 16,800$ and $Ra_c^{sup} = 20,200$. Thus, the gravitactic convection is subcritical. This was not the case in cylindrical enclosure in which it was supercritical [14]. For $Pe = 1$ shown in Fig. 2b, it appears that the gravitactic convection is subcritical at $Ra_c^{sub} = 1730$ and its value is reduced

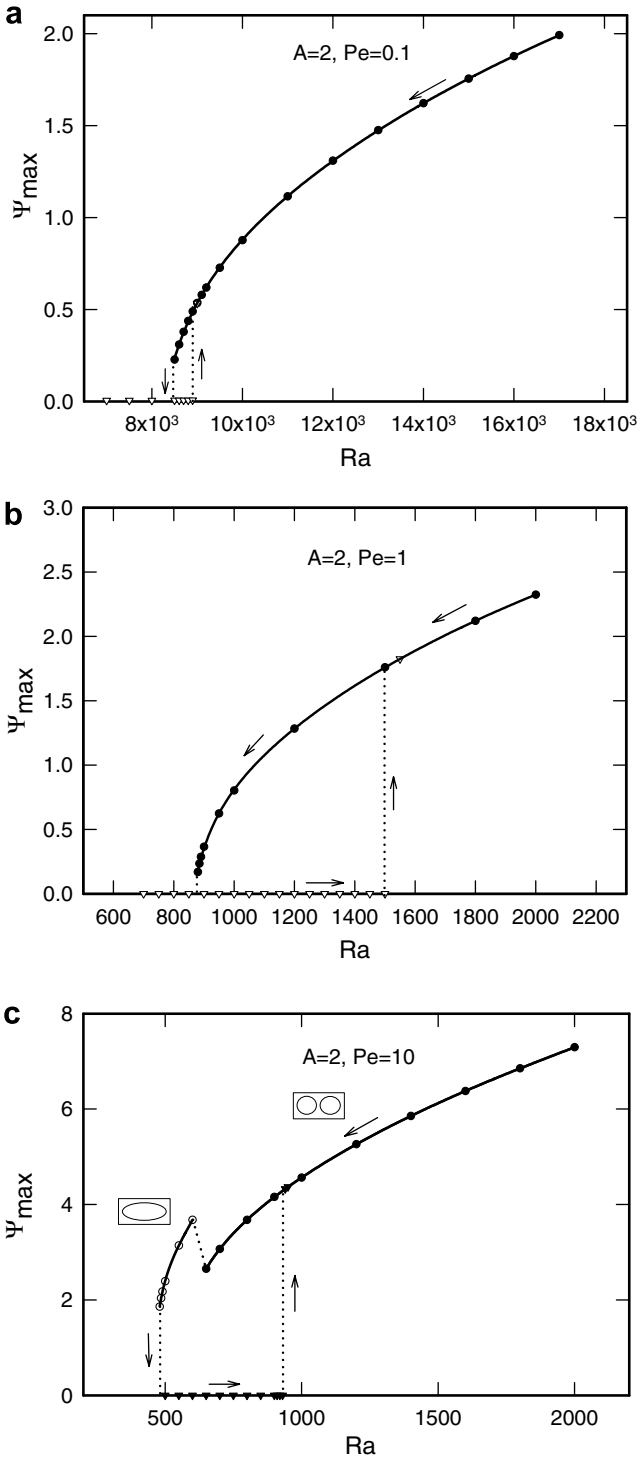

Fig. 4. Bifurcation diagrams for aspect ratio $A = 2$ and various bioconvection Peclet numbers. (a) $Pe = 0.1$, (b) $Pe = 1$ and (c) $Pe = 10$.

considerably by increasing Pe number from 0.1 to 1. We have a supercritical $Ra_c^{sup} = 1770$ from the diffusive state. The solution is unstable as shown in Fig. 2b. When we further increase Pe number to 10, we see in Fig. 2c that a similar situation is obtained as for $Pe = 1$, i.e., we have a subcritical bifurcation and Ra_c^{sub} is further decreased with increasing bioconvection Pe number. The convection sets in at a supercritical Rayleigh number of $Ra_c^{sup} = 800$, which is obtained from the diffusive state.

We present in Fig. 3 streamlines and isoconcentration at Rayleigh numbers slightly above the critical Rayleigh number for each case of Fig. 2, i.e., for $Pe = 0.1$, $Ra = 17{,}000$, $Pe = 1$, $Ra = 1780$ and $Pe = 10$, $Ra = 780$. We see the strong influence of Peclet number on the concentration field: for $Pe = 0.1$, the micro-organism concentration is uniform in the enclosure, for $Pe = 1$, it is similar to that of $Pe = 0.1$ with some accumulation on the top, and as Peclet is further increased to 10, the micro-organisms are accumulated on the top. The flow patterns show that the fluid flow covers almost all the enclosure regardless of Peclet number.

The results of the case with $A = 2$ and $Pe = 0.1$, 1, 10 are shown in Fig. 4. We see that the gravitactic convection is subcritical with all three Pe numbers. For $Pe = 0.1$ in Fig. 4a, $Ra_c^{sub} = 8400$, which is smaller than the critical Rayleigh obtained for $A = 1$ for the same Pe number. For $Pe = 1$ shown in Fig. 4b, $Ra_c^{sub} = 870$ and for $Pe = 10$ shown in Fig. 4c, $Ra_c^{sub} = 455$. Also in all these cases the critical Rayleigh number is lower than those for the case with $A = 1$. We note that for $Pe = 10$, when the results obtained from the convective state, we have two convection cells from $Ra = 2000$ down to 650 at which the flow field changes to one cell. Similarly, in the case of the result obtained from the diffusion state, the supercritical Rayleigh number is 930 at which we get directly a flow field with two convection cells.

We present in Fig. 5 the flow and concentration fields at $Ra = 2000$, 650 and 600. At $Ra = 2000$ in Fig. 5a, the flow field is with two cells, the right one is counterclockwise and the left clockwise rotating, as a result, the fluid sinks at the center of the enclosure. The micro-organisms are concentrated at the top center. At $Ra = 650$ shown in Fig. 5b, the flow field is similar to the one in Fig. 5a, however, with reduced circulation strength. As a result, we have a similar isoconcentration pattern. At $Ra = 600$ in Fig. 5c, we have a single counterclockwise circulating cell at the left upper corner and the micro-organisms form a layer at that corner.

We present the shallow enclosure case, $A = 5$ with Pe from 0.1 to 10 in Fig. 6. For $Pe = 0.1$ in Fig. 6a we have a subcritical bifurcation at $Ra_c^{sub} = 6990$. The gravitactic convection obtained from the convection state is with the flow field having four cells from $Ra \sim 50 \times 10^3$ down to 13,000, then the flow field becomes with two convection cells, Ra from 12,000 down to 6990. By continuing at lower Ra numbers, the convection disappears suddenly at 6990. Starting with diffusive state, we obtain the supercritical Rayleigh number, $Ra_c^{sup} = 9600$, slightly above which, the gravitactic convection begins with two convection cells.

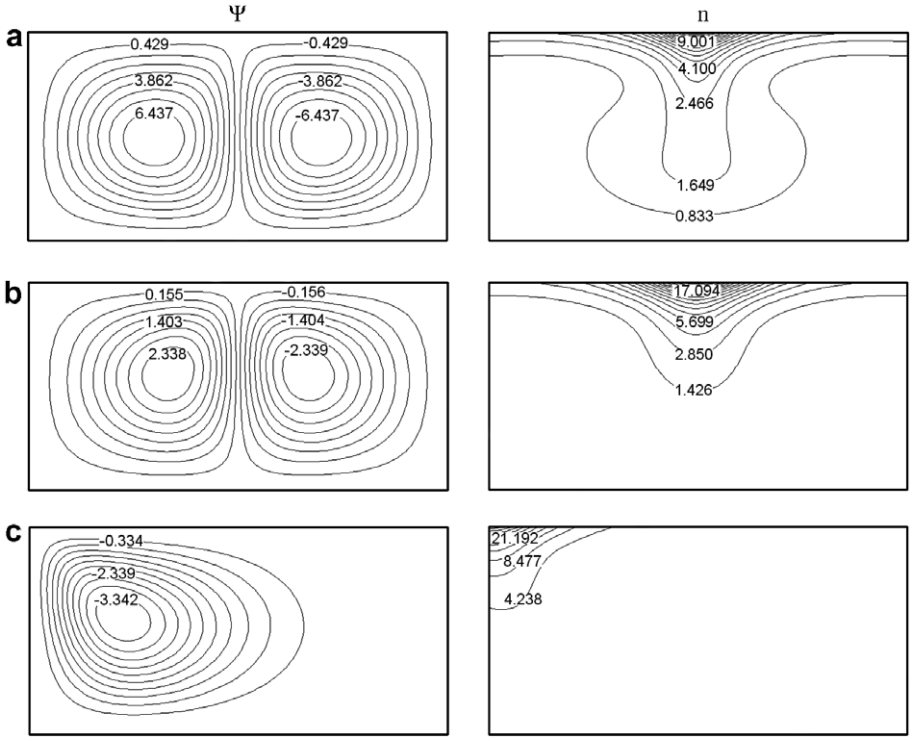

Fig. 5. Isolines for $A = 2$ and $Pe = 10$ of bifurcation diagram in Fig. 4c at various Rayleigh numbers. (a) $Ra = 600$, (b) $Ra = 650$ and (c) $Ra = 2000$. Streamlines are shown on the left and isoconcentration on the right.

For $Pe = 1$ shown in Fig. 6b, we have a subcritical bifurcation. The gravitactic convection obtained from the convection state is with four cells. By continuing at lower Rayleigh numbers, the flow with three cells is obtained at Rayleigh about 1200 down to 950. Then, the flow becomes with two cells at $Ra = 905$. By continuing still at lower Ra numbers, the two cells convection becomes one cell convection at $Ra = 870$. Then, the convection disappears at Rayleigh number, $Ra_c^{sub} = 775$. Starting from the diffusive state, we have a supercritical Rayleigh number at $Ra_c^{sup} = 1450$, above which we obtain convection with three convection cells, yet at the same Rayleigh number, we obtained four convection cells in case of starting from the convection state. As discussed before, this is due to unstable convective flow.

To see these different states, we plotted streamlines and isoconcentration, and presented in Fig. 7 to illustrate the flow and concentration fields thus obtained corresponding to various states observed in Fig. 6b. For $Ra = 2000$ shown in Fig. 7a, we see four convection cells and the concentration varies in a way corresponding to the cells formed. The right cell is clockwise, the next two cells in the central part are counterclockwise and clockwise circulating and the last cell at the left is counterclockwise circulating. Thus, the micro-organisms are concentrated on the top at the left and right corners and at the center above the two convection cells in the center. For $Ra = 1200$ in Fig. 7b, we have three convection cells formed. The right cell is clockwise circulating as a result of which the micro-organisms are concentrated on the top at the right corner. As the left cell circulating clockwise and the center one counterclockwise, they are concentrated on top of the two left cells. At $Ra = 900$ in Fig. 7c, we see the micro-organisms are concentrated at the top corners corresponding to clockwise circulating right cell and counterclockwise circulating left cell. At $Ra = 780$ in Fig. 7d we have a flow with single clockwise circulating convection cell squeezed to the right, the micro-organisms are concentrated at the top right corner.

As Pe increased to 10, shown in Fig. 6c, the bifurcation is subcritical at $Ra_c^{sub} = 250$. The solution obtained from the convection state is with six cells. By continuing at lower Rayleigh numbers, the flow with four cells is obtained at Rayleigh about 1150 down to 920, and then with two cells at 900 down to 505. At still lower Ra numbers, the convection becomes single cell at 450 and it disappears at $Ra_c^{sub} = 250$. Starting from the diffusive state, the bifurcation is supercritical at $Ra_c^{sup} = 920$, above which we obtain convection with four cells. The influence of Peclet number at various Rayleigh numbers in this case is shown in Fig. 8. At $Ra = 1500$ in Fig. 8a, the flow field is with six cells and the isoconcentration follows the pattern of each pair of convection cells: the micro-organisms are accumulated at the top location corresponding to the sinking fluid of each pair. At $Ra = 1000$ in Fig. 8b, the flow field is with four cells. The right and left cells rotate clockwise and counterclockwise, respectively, and as a result, the micro-organisms are accumulated at the left and right corners at the top. At the center, the fluid sinks at the center by the counterclockwise and clockwise rotating pair of cells and we see the micro-organisms are accumulated at the top center. At $Ra = 700$ in Fig. 8c, there are two convection cells, the right one clockwise and the left one counterclockwise rotating. The micro-organisms are accumulated at the top

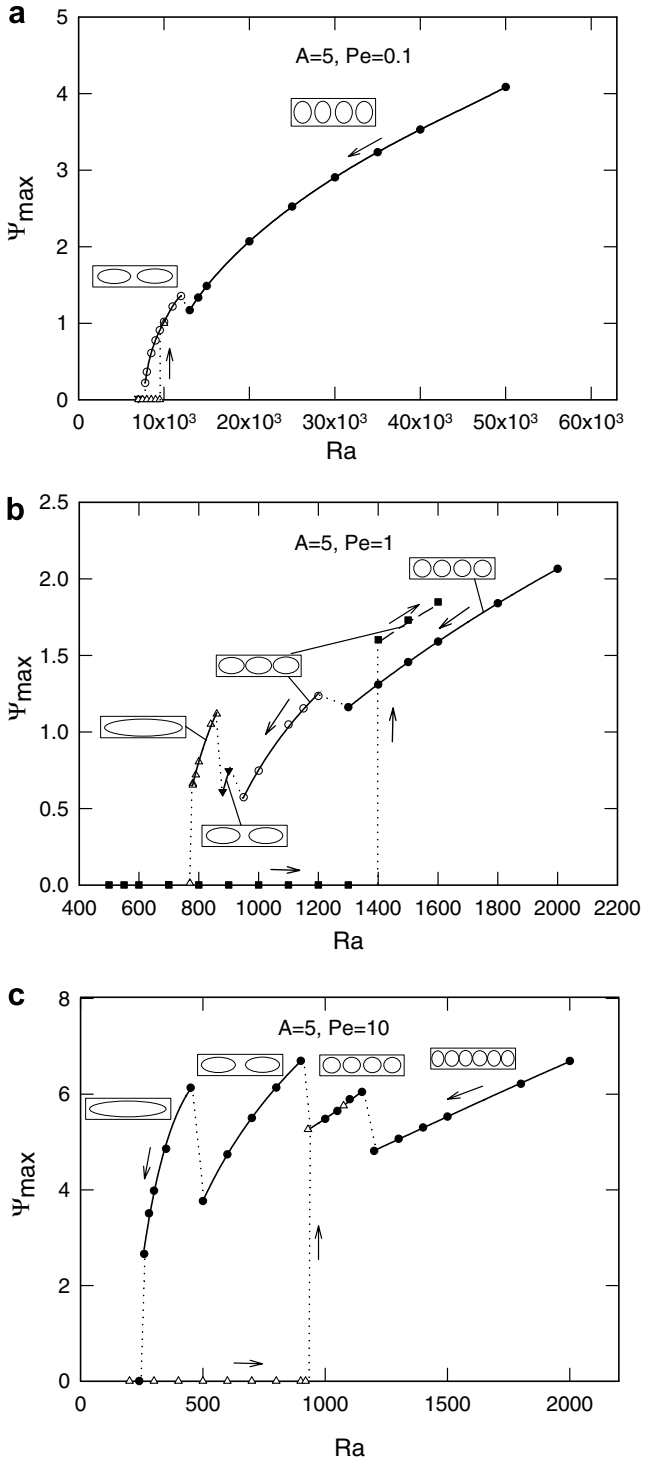

Fig. 6. Bifurcation diagrams for aspect ratio $A = 5$ and various bioconvection Peclet numbers. (a) $Pe = 0.1$; (b) $Pe = 1$ and (c) $Pe = 10$.

corners. At $Ra = 300$ in Fig. 8d, just above Ra_c^{sub}, the flow field becomes with a clockwise rotating single cell and the whole micro-organisms are accumulated at the right corner.

For $Pe = 1$ and 10 in Fig. 6b and c, the convective flow in the region between Ra_c^{sup} and Ra_c^{sub} is unstable where, depending on the Rayleigh number, different convection patterns are formed. In fact, we see in Fig. 6b and c and the corresponding patterns in Fig. 8 that the number of convection cells formed changes from 4 to 2 and from 2 to 1 before reaching the sub-critical Rayleigh number.

To see the mechanism of pattern change near super critical Rayleigh number of Fig. 6c, we present the time sequence diagrams at $Ra = 1000$, 900 and 800 in Fig. 9. Following the procedure explained earlier, we obtained the solution at $Ra = 1000$ by using the solution from the previous solution at $Ra = 1050$ from which we get ($t = 0.02$, $\psi_{ext} = 5.634$). We see in Fig. 9a that after a relatively short computation time ($t = 0.75$, $\psi_{ext} = 5.542$), the solution becomes quasi steady-state, a typical time sequence. After satisfying the convergence criteria Eq. (14), we obtain ($t = 12.26$, $\psi_{ext} = 5.5424$, $Ra = 1000$), which is on the bifurcation curve with four convection cells. To obtain solution at $Ra = 900 < Ra_c^{sup} = 920$, we follow the same procedure and use the solution at $Ra = 1000$. The time sequence diagram is shown in Fig. 9b; in a very short computation time at ($t = 0.02$, $\psi_{ext} = 5.3202$), ψ_{ext} increases steadily from ($t = 0.30$, $\psi_{ext} = 5.0108$) to ($t = 762$, $\psi_{ext} = 5.6219$), and then it increases suddenly to ($t = 768$, $\psi_{ext} = 6.6725$) and finally a converged solution is obtained at ($t = 833$, $\psi_{ext} = 6.6935$, $Ra = 900$), at which we have a pattern of two convection cells. The next computation at lower

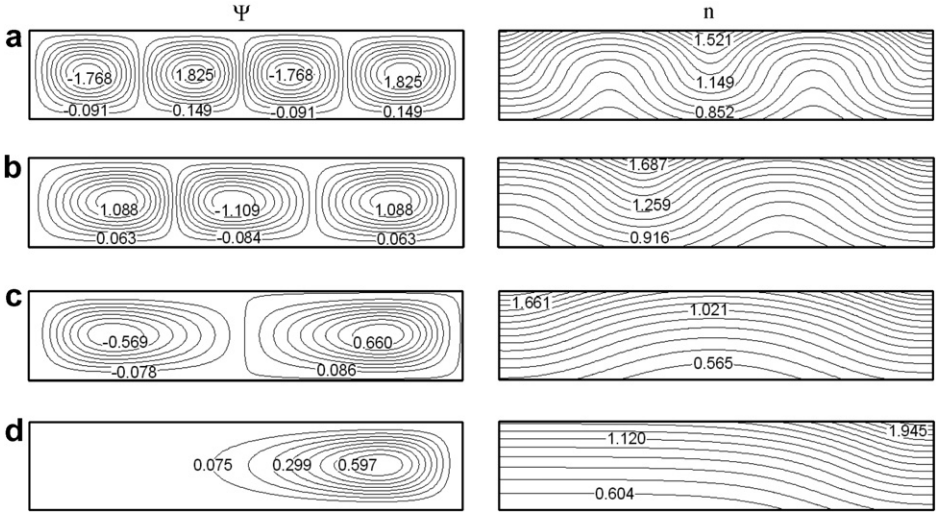

Fig. 7. Isolines for $A = 5$ and $Pe = 1$ of bifurcation diagram in Fig. 6b at various Rayleigh numbers. (a) $Ra = 2000$; (b) $Ra = 1200$; (c) $Ra = 900$ and (d) $Ra = 780$. Streamlines are shown on the left and isoconcentration on the right.

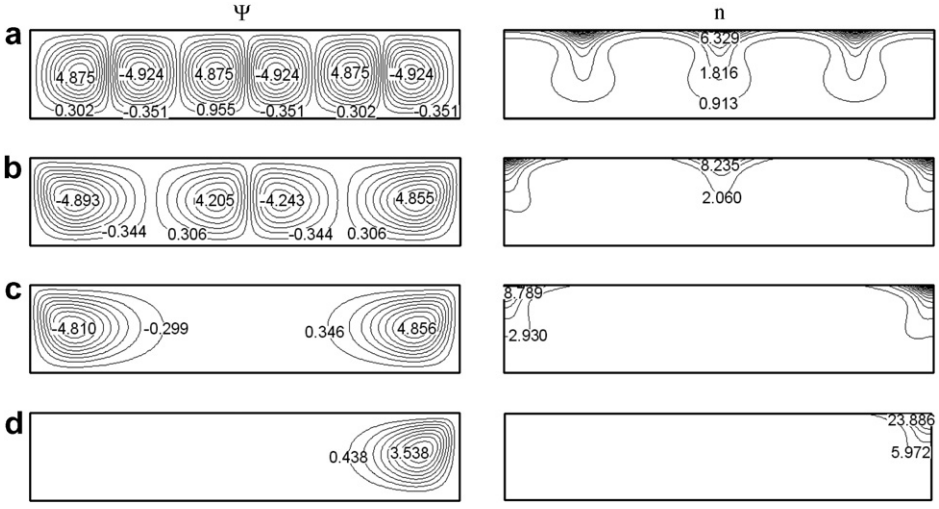

Fig. 8. Streamline and isoconcentration patterns at various Rayleigh numbers of Fig. 6c for $A = 5$, $Pe = 10$. (a) $Ra = 1500$; (b) $Ra = 1000$; (c) $Ra = 700$ and (d) $Ra = 300$.

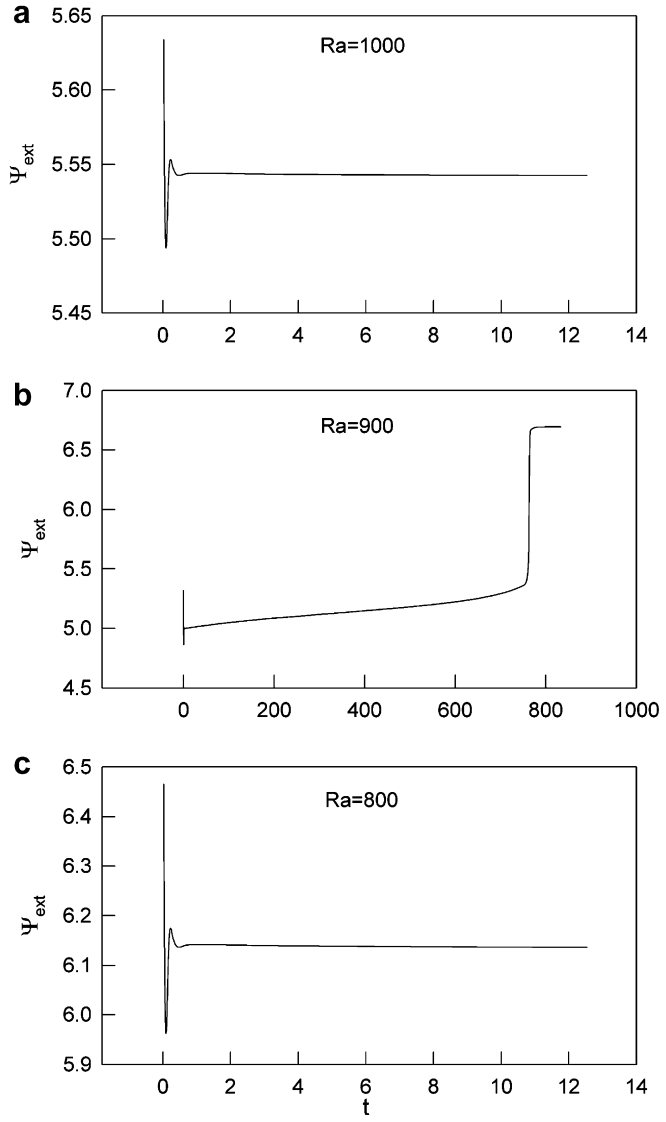

Fig. 9. Time sequence diagrams corresponding to the case with $A = 5$, $Pe = 10$ of Fig. 6c at (a) $Ra = 1000$; (b) $Ra = 900$ and (c) $Ra = 800$.

$Ra = 800$ is done similarly by reading the solution from $Ra = 900$, the time sequence diagram of which is shown in Fig. 9c. We observe that the time sequence is once more a typical one, like in Fig. 9a, and the solution is ($t = 12.54$, $\psi_{ext} = 6.1363$, $Ra = 800$) with two convection cells. We note that the mechanism of pattern formation observed here is quite different from that of gyrotactic bioconvection in narrow and tall enclosures [9].

5. Conclusion

Numerical simulations of gravitactic bioconvection in rectangular enclosures were carried out. The vertical walls of the cavity are assumed to be stress-free and insulated, while horizontal boundaries are rigid. The governing equations are integrated numerically using the control volume method. The present results exhibit the influence of bioconvection Peclet number and aspect ratio on the bifurcation diagram and the flow structure. We have found that the bifurcation remains subcritical in all cases when the bioconvection Pe number is varied from 0.1 to 10 in rectangular enclosures having an aspect ratio from 1 to 5.

Acknowledgement

The financial support for this study by Natural Sciences and Engineering Research Council Canada is acknowledged.

References

[1] A.M. Metcalfe, T.J. Pedley, Falling plumes in bacterial bioconvection, J. Fluid Mech. 445 (2001) 121–149.
[2] A.J. Hillesdon, T.J. Pedley, Bioconvection in suspensions of oxytactic bacteria: linear theory, J. Fluid Mech. 324 (1996) 223–259.
[3] N.A. Hill, T.J. Pedley, J.O. Kessler, The growth of bioconvection patterns in a suspension of gyrotactic micro-organisms in a layer of finite depth, J. Fluid Mech. 208 (1989) 509–543.
[4] T.J. Pedley, J.O. Kessler, Hydrodynamic phenomena in suspensions of swimming micro-organisms, Ann. Rev. Fluid Mech. 24 (1992) 313–358.
[5] N.A. Hill, T.J. Pedley, Bioconvection, Fluid Dynam. Res. 37 (2005) 1–20.
[6] S. Childress, M. Levandowsky, E.A. Spiegel, Pattern formation in a suspension of swimming micro-organisms: equations and stability theory, J. Fluid Mech. 63 (1975) 591–613.
[7] S. Fujita, M. Watanabe, Transition from periodic to non-periodic oscillation observed in a mathematical model of bioconvection by motile micro-organisms, Physica D: Nonlinear Phenomena 20 (1986) 435–443.
[8] A. Harashima, M. Watanabe, L. Fujishiro, Evolution of bioconvection patterns in a culture of motile flagellates, Phys. Fluids 31 (1988) 764–775.
[9] S. Ghorai, N.A. Hill, Development and stability of gyrotactic plumes in bioconvection, J. Fluid Mech. 400 (1999) 1–31.
[10] T.J. Pedley, N.A. Hill, J.O. Kessler, The growth of bioconvection patterns in a uniform suspension of gyrotactic micro-organisms, J. Fluid Mech. 195 (1988) 223–237.
[11] S. Ghorai, N.A. Hill, Wavelengths of gyrotactic plumes in bioconvection, Bull. Math. Biol. 62 (2000) 429–450.
[12] M.A. Bees, N.A. Hill, Non-linear bioconvection in a deep suspension of gyrotactic swimming micro-organisms, J. Math. Biol. 38 (1999) 135–168.
[13] S. Childress, E.A. Spiegel, Pattern formation in suspension of swimming micro-organisms: nonlinear aspects, in: D. Givoli, M.J. Grote, G.C. Papanicoulao (Eds.), A Celebration of Mathematical Modeling: The Joseph B. Keller Anniversary Volume, Kluwer, Dordrecht, 2004, pp. 33–52.
[14] Z. Alloui, T.H. Nguyen, E. Bilgen, Bioconvection of gravitactic micro-organisms in vertical cylinder, Int. Commun. Heat Mass Transfer 32 (2005) 739–747.
[15] S.V. Patankar, Numerical Heat Transfer and Fluid Flow, McGraw Hill, New York, 1980.
[16] A. Pellew, R.V. Southwell, On maintaining convective motion in a fluid heated from below, Proc. Royal Soc. Series A, Math. Phys. Sci. 176 (1940) 312–343.
[17] T. Kawakubo, Y. Tsuchiya, Diffusion coefficient of paramecium as a function of temperature, J. Protozool. 28 (3) (1981) 342–344.
[18] Y. Mogami, A. Yamane, A. Gino, S.A. Baba, Bioconvective pattern formation of Tetrahymena under altered gravity, The J. Exp. Biol. 207 (2004) 3349.